

International Conference on Computational Science, ICCS 2013

Multiscale Agent-based Model of Tumor Angiogenesis

Megan M. Olsen^{a,*}, Hava T. Siegelmann^b

^aLoyola University Maryland, 4501 N. Charles St., Baltimore, MD 21210, USA

^bUniversity of Massachusetts Amherst, 140 Governors Dr., Amherst, MA 01003, USA

Abstract

Computational models of cancer complement the biological study of tumor growth. However, existing modeling approaches can be both inefficient and inaccurate due to the difficulties of representing the complex interactions between cells and tissues. We present a three-dimensional multiscale agent-based model of tumor growth with angiogenesis. The model is designed to easily adapt to various cancer types, although we focus on breast cancer. It includes cellular (genetic control), tissue (cells, blood vessels, angiogenesis), and molecular (VEGF, diffusion) levels of representation. Unlike in most cancer models, both normally functioning tissue cells and tumor cells are included in the model. Tumors grow following the expected spheroid cluster pattern, with growth limited by available oxygen. Angiogenesis, the process by which tumors may encourage new vessel growth for nutrient diffusion, is modeled with a new discrete approach that we propose will decrease computational cost. Our results show that despite proposing these new abstractions, we see similar results to previously accepted angiogenesis models. This may indicate that a more discrete approach should be considered by modelers in the future.

Keywords: multiscale; agent-based; computational biology; tumor growth; angiogenesis

1. Introduction

Cancer incidence is expected to rise worldwide from 12 million new people affected annually in the year 2000 to an anticipated 20 million in the year 2030. Not only are more people being diagnosed each year (adjusted to a standard population size), but there are also more total deaths from cancer. The only disease that is currently more deadly than cancer is heart disease; but in five years cancer is expected to be top of the list for the first time.

With the use of computational and mathematical models we can examine how biological systems like cancer work in multiple scales, as well as create new testable hypotheses [1]. As with simulation models in general, these models must be based on biological knowledge and data and validated before their results can be used to direct biological research. Although there is great promise from computational and mathematical techniques for cancer research, the cancer biology community is still in the process of accepting the potential of these models [2]. Improved model approaches will increase their trust in this approach, and is part of the goal of this work.

Modeling biological systems such as cancer allows us to analyze them in a different way than is traditionally done by biologists. Ideally, biologists and modelers work together to form a complete cycle where biological experiments feed into computational/mathematical models, which then feed back into the biological experiments to continue the cycle[3]. Both fields are still working to achieve this collaboration and balance. Ideally, models

*Corresponding author. Tel.: +1-410-617-2852 ; fax: +1-410-617-2157.
E-mail address: mmolsen@loyola.edu.

are used for their predictive power such as is currently attempted in epidemiology for predicting the spread of disease with and without vaccines [4].

Many different types of models are used to study biological problems, which are usually complex systems: ordinary differential equations (ODE), partial differential equations (PDE), agent-based simulations, event-based simulations, cellular automata, computational geometry, and more. We introduce a three-dimensional multiscale agent-based model and simulation of cancer cell growth that incorporates the growth of new blood vessels necessary to support that growth (angiogenesis). It has been suggested that three dimensional models have the most to offer for bridging the gap between in vivo studies in two-dimensional cultures and the larger animal system [1]. Agent-based models allow each cell to be modeled separately, following some series of rules on its behavior. Our model abstracts the complex environment of cancer development and progression, and examines it on three scales: molecular, cellular, and tissue. Although previous agent-based models of cancer growth have been developed, as have previous models of angiogenesis, these two approaches are rarely combined in a single model. We show that by using a multiscale agent-based approach, we can represent complex nutrient flow and angiogenesis with similar results to previous models, despite increasing efficiency through increased abstraction. This new approach to modeling nutrient flow may allow more robust and time efficient modeling in the future. In the next section we will discuss additional related work, then describe the model, followed by results, and conclusions.

2. Related Work

2.1. Cancer Background

Cancer is essentially a disease in which certain cells no longer follow the originally defined genetic rules. Hanahan and Weinberg defined a set of six properties that represent the failures needed within a cell for it to become cancerous [5]. All failures occur via mutations to the cell's DNA, caused by proliferation, i.e. the creation of a daughter cell, or a variety of other mechanisms. However, not all orderings of mutations will result in a cancer cell. Since cells are generally able to repair damage to their DNA, or undergo apoptosis (self-death) if repair fails, the ability to repair genetic mutations and the ability to undergo apoptosis must be some of the first mutations to be sustained. Afterward, the cell must become mutated in the tumor suppressor genes (e.g. p53), as otherwise the detrimental effects of increased growth will not occur. Next, the cell may be mutated in the ability to proliferate such that its proliferation is increased. This may include multiple mutations as the rate of proliferation is controlled in multiple ways. Mutations in a different order will not create a cancer cell, but instead will create a cell that will undergo either repair or apoptosis (self-death) to maintain the system [6, 7].

With these mutations the cell has accomplished four of Hanahan and Weinberg's requirements. Tumor growth is monitored by many processes, including the diffusion of nutrients. A tumor cluster will slow its growth as nutrients become scarce. As nutrients are depleted by the tumor, the cells that do not receive enough nutrients to function normally will be in one of two states: necrotic or hypoxic. A hypoxic cell receives enough nutrient to continue surviving, but not enough to proliferate. A cell may remain hypoxic indefinitely. A necrotic cell is a cell that has received even fewer nutrients, such that it does not receive enough nutrients to survive. Once a cell becomes necrotic, there is no way to revive it; it will eventually die.

Tumor cells, however, are often able to convince nearby vasculatures to grow such that the tumor can receive enough nutrient to continue growing. This process is called angiogenesis, and is different from the growth of new blood vessels during normal development. Hypoxic tumor cells emit chemicals such as VEGF into the environment. Once these chemicals meet a vasculature, they can encourage the growth of endothelial cells for the creation of new vasculatures. These sprouts will only provide nutrient to the tumor once they have created a loop so that blood can flow. Without angiogenesis, a tumor's development will be limited, so angiogenesis is necessary to sustain continued growth. Additionally, angiogenesis is necessary to properly model the growth of the tumor, as otherwise growth is incorrectly limited.

2.2. Cancer Models

There are many valid techniques for studying cancer; the choice of spatial vs. non-spatial (such as an ODE) model can have a huge impact on the results. We choose to utilize a spatial representation of cells as it is more similar to the original biological system and thus allows for the inclusion of a greater number of detailed aspects.

To explicitly represent space the primary options are partial-differential equations (PDE), a cellular automata model, or an agent-based model. We choose to use agent-based models as they are particularly well suited for examining multiple scales. They also have the benefit of being able to be simulated in a more accurate way than how one would simulate a PDE. As there are not a significant number of agent-based angiogenesis models, we will discuss general agent-based cancer models, as well as spatial angiogenesis models.

CancerSim, a three-dimensional agent-based model, begins with a cancer-free system and then models the growth of the cancerous cells based on the hallmarks of cancer [5, 8]. It therefore takes into account basic cellular properties such as genetic instability, telomere length, and random apoptosis. Another three-dimensional agent-based tumor model utilizes basic gene-protein interactions and multi-cellular patterns specific to brain cancer [9]. This model represents internal cellular processes via differential equations, and the location of cells spatially.

However, neither of the above models incorporate angiogenesis. Models of angiogenesis fall into three categories: models of vasculature growth without tumor or other tissue cells, models of vasculature growth with only tumor cells, and models of vasculature growth with both tumor and healthy tissue cells. Generally, models of angiogenesis include the growth of vasculatures to support tumors and the size of tumors with and without angiogenesis. In some models angiogenesis is just one of the mechanisms modeled in order to answer a different question, such as the shape of growth or time of growth of the tumor.

Various levels of mathematical modeling exist to include how capillaries are formed, the flow of blood, vessel adaptation, and the extent of which chemical diffusion reaches the tissue. McDougall et al. analyze how drugs can be sent to the tumor via the formed vessel network, based on the quality of the created vessels. They found that the simulation was sensitive to changes in parameters for haptotactic response of the blood vessel cells, blood viscosity, and blood pressure, and that the tracer-drug sent through the system was able to travel easiest through the well formed vessels [10]. A discrete mathematical model based on PDEs has been used to examine the spatio-temporal evolution of capillary networks in two and three dimensions [11]. Capillaries grow by following the gradient of TAF. They find that the model provides capillaries with realistic structure and morphology.

A two-dimensional multi-scale model of angiogenesis where endothelial cell sprouting occurs due to VEGF diffused by healthy cells in an initial development phase, and by tumors that are later implanted into the model, has been developed [12]. Sprouts grow based on VEGF gradient that occurs when cells do not have enough oxygen. Sprouts die if they do not create a loop within a given period of time, and are only active once it is a viable segment. They find that a larger number of tumor cells causes a higher vascular density, and that network remodeling requires a balance between angiogenesis and vessel pruning. A two-dimensional PDE model of tumor growth with angiogenesis has also been developed [13]. They find that asymmetrical tumor growth leads to a greater degree of branching at the surface of the tumor when compared to symmetrical tumor growth.

Multiple angiogenesis models are based on the cellular Potts model. One such model found that sprout morphology is not affected by how far from the tip the proliferating region is, although the speed of growth is affected [14]. Another Potts model analyzes tumor growth with and without angiogenesis [15]. The initial vasculature is represented as a grid. Endothelial sprouts grow in biased random movement toward VEGF secreted by hypoxic tumor cells, with the only modeled nutrient being oxygen. They find that the system goes through six phases of growth, and that their results are similar to other models. We include similar aspects in our model, although we use a different level of abstraction, and thus will compare our results to [15].

Cellular automata models are also used to investigate branching properties of vessels. Some models focus on branching rules and how they change the vasculature, with a brief description of how it may be applied to tumor angiogenesis [16]. Others focus specifically on tumor angiogenesis, with either a visual comparison to in vivo endothelial sprouting [17] or a comparison with data on in vivo vascular growth [18]. Both find that their sprouting is similar to what would be expected from tumor angiogenesis.

None of the above models consider how the cancer cells affect the rest of the system, however. An agent-based approach can be used to investigate the role of the immune system in reacting to and fighting tumor growth, which includes immune cells in addition to tumor cells [19]. We design our model to include healthy tissue cells instead of the immune cells. Including other types of cells leads to a more realistic model, as surrounding cells have already been shown to play a role in affecting cancer growth. The agent-based model described in this paper is designed to incorporate many aspects of cancer growth including angiogenesis, but with algorithmic choices that allow a complex model to still be able to be run in only a few hours. We hypothesize that multiscale agent-based modeling is the desired next direction in cancer growth modeling.

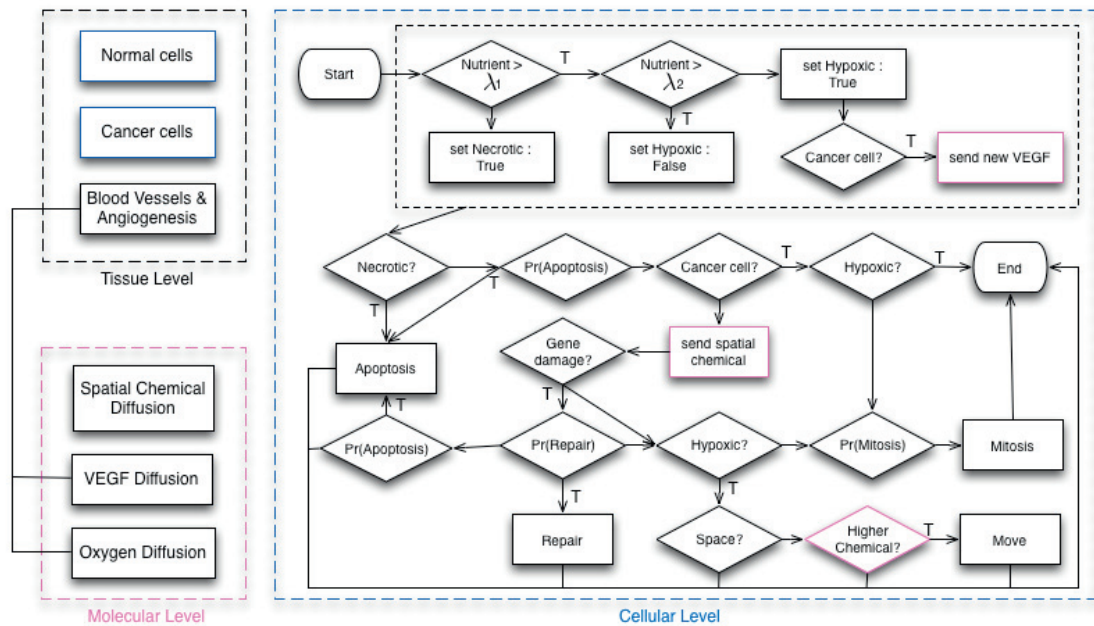


Fig. 1. Model overview with the basic relationships between the three scales, including a cellular level flow chart of agent decisions for both normal and cancer cells, for every time step. Normal and cancer cells also differ by what probabilities are used for decisions. Angiogenesis is modeled both at the tissue level (branching of new sprouts) and at the molecular level (diffusion of oxygen and VEGF).

3. Modeling Approach

Each agent represents a single cell, and exists on a three-dimensional grid to approximate a tissue. The system is modeled on three scales (Figure 1): molecular (VEGF, diffusion), cellular (genes, space) and tissue (vasculatures, branching). Although two-dimensions can also be modeled, three dimensions provides a more realistic representation. Agents follow individual “life protocols” defined and implemented through probabilities represented within their computational genes. We consider normal tissue cells to be of size $10\mu\text{m}$, and each time step to represent approximately one day. Vasculatures in the system give agents nutrients, which they require to survive. Without tumor growth, the system can self-maintain essentially forever. The basic agent architecture is based on [20].

3.1. Genes and the Life Protocols

The basic life protocols are based on Hanahan and Weinberg’s hallmarks of cancer [5], and thus reflect proliferation (including rate parameters, generation potential, and space restrictions [21, 22, 23]), proliferation-suppression mechanisms, self-testing at a check point prior to the replication decision, repairing damage, and apoptosis (self-death). The latter is activated as a random process, secondary to an agent’s decision to die due to aging or uncorrected defects. The distance regulation protocol maintains shape cohesiveness and allows undisturbed communication flow among agents [24]. These protocols are chosen to approximate the healthy functioning of phenotypic properties of cycling cells. A flow chart of the decisions by a cell at every time step can be seen in Figure 1.

Tumor agents develop in the system when all of an agent’s life protocols are damaged. A tumor agent can only produce tumor agents and cannot back mutate into a normal agent. Since all life protocols are broken, a tumor’s ability to follow each of those protocols is also broken: it is not able to repair the mutations, it cannot undergo apoptosis that would occur due to mutations, and it proliferates more frequently than a healthy cell.

The life protocols of the cells are based on the life protocols in [25], where further details can be found. This work enhances the cellular modeling of that work by the addition of nutrients and angiogenesis to the model. We do not include the rescue protocols.

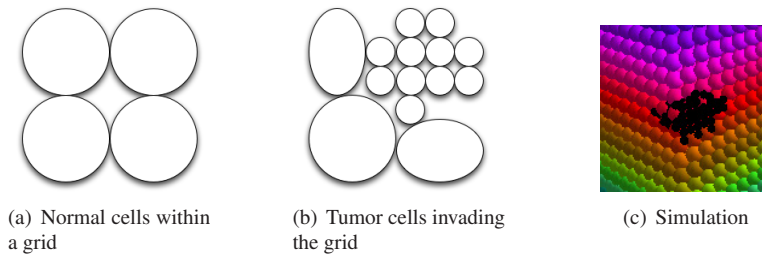


Fig. 2. Relative size of normal and tumor cells at the tissue level, in 2D for easier viewing. (a) Normal cells are by default larger, (b) but are resized as tumor cells push their way into the system. (c) In the simulation, tumor cells are shown in black and normal cells are colored. Although cells are not spherical *in vivo*, this abstraction allows for reasonable modeling without altering results.

3.2. Spatial Representation

Three-dimensional space is represented by a grid. Normally functioning tissue cells generally require more space than tumor cells (Figure 2). Our model abstracts this necessity by assuming normal cells to be twice the size of tumor cells. Their location is determined by a set of coordinates (x,y,z) that define their center point. With no neighboring tumor cells, the cell retains a radius of 1.5 grid locations. Thus, you can consider each normal cell to be on every other lattice point.

A spatial chemical is also diffused by each cell. This chemical allows normally functioning cells to determine in what direction the highest proportion of cells exists within their larger neighborhood. If a cell is moving, it will move toward the highest chemical amount as that indicates the mass of the tissue as opposed to the edge. This spatial chemical enables normal cells to grow in a spheroid initially as they populate the system prior to any tumor cell creation.

The addition of tumor cells disrupts this status quo. A tumor cell also has a coordinate (x,y,z) but only a radius of 0.5 grid locations. Thus, for every normal cell, there may be 27 tumor cells. However, it will take some time before tumor cells proliferate in such a way that normal cells become reduced to this smaller size. A reduction in space affects a normal cell's ability to proliferate and move.

3.3. Nutrients: Oxygen

All cells require nutrients to survive, which they acquire from blood vessels. We specifically model oxygen as it is generally the most limiting nutrient sent to cells. Each blood vessel diffuses nutrients to nearby agents in all directions. There is a limited amount of nutrient that can be supplied by a single vessel, and a limited distance that it can travel from the vessel. Additionally, as agents use nutrient it decreases the amount of nutrient available for agents further from the vessel. Thus, vessels must occur close enough to sustain all agents, but optimally should be as far apart as possible to accomplish that goal.

We represent blood vessels at equidistant locations throughout the tissue (every $200\mu m$ since oxygen can diffuse up to $100\mu m$), forming a grid. We further view the grid as creating a series of compartments, with each compartment being bounded on three sides by vessels, one in each of the three directions. These vessels can supply nutrients to all healthy cells within the tissue, assuming there are no tumor cells present. Nutrients are distributed to cells from each vessel, first to the cells closest to the vessel, then to the next layer of cells past that, etc, until the maximum number of cells that vessel can support has been reached in each of the three dimensions surrounding it. We assume blood flows from the zero location to the maximum location for each vessel. Each vessel also has a maximum number of cells that can be supported overall in the model, in addition to the maximum amount within each region. Thus, if a region closer to the beginning of the tissue has additional cells that use more oxygen, the cells further along the vessel will be more likely to become hypoxic.

This technique for representing vessels and their flow is unique among angiogenesis models. Other models have utilized a grid, but they rely on specific calculations at every location for the amount of nutrient available. To decrease the complexity in the model, instead of explicitly modeling the diffusion process we model the effect of diffusion. Usually diffusion is modeled using PDEs that must then be solved to determine the amount of gradient available at every location within the grid. Even discretizing this using standard grid diffusion techniques

Algorithm 1 Diffusion of nutrients

```

1: compartmentNutrientMax
2: vesselNutrientMax = compartmentNutrientMax * numberOfCompartments
3: for each compartment in vessel do
4:   availableNutrient = compartmentNutrientMax
5:   for each diffusion radius within diffusionRadiusMax do
6:     for each location from 0 to compartmentWidth at this radius do
7:       if availableNutrient < 0 then
8:         availableNutrient = 0
9:       end if
10:      send availableNutrient to each of N cells at location
11:      availableNutrient = availableNutrient - N
12:    end for
13:  end for
14: end for

```

becomes computationally expensive due to the fact that the amount of nutrient available to a cell not only relies on the amount of nutrient in its location, but also on how many cells have taken nutrient from the environment before the nutrient reaches that cell. Thus, the diffusion also relies on the number of cells between a cell and its closest vessels. To take this issue into account, we instead do a stepwise diffusion from each vessel as seen in Algorithm 1. The *compartmentNutrientMax* is defined as in Equation 1. α represents the number of direct neighbors in $numDimensions - 1$ (in the case of three-dimensions, $\alpha = 8$). The *diffusionRadiusMax* is defined as *compartmentHeight*/2.

$$compartmentNutrientMax = \sum_i^{compartmentHeight} (\alpha * i) * compartmentLength \quad (1)$$

Cells that receive enough nutrients are considered normal and function as described previously. It is expected that cells will receive nutrients from three vessels: one in the X direction, one in the Y direction, and one in the Z direction. Thus, the minimum amount of nutrient for a cell to remain normal is three times what each vessels should give them (λ_1). Cells that receive nutrients but not enough to remain normal (λ_2) will become hypoxic, and thus unable to proliferate until the nutrients increase again. Cells can return from the hypoxic state to a normal state each time step, if their nutrients are $> \lambda_1$. Cells that receive zero nutrients will become necrotic and die immediately.

3.4. Angiogenesis

Angiogenesis is the creation of new blood vessels, as described in section 2. In the model, all hypoxic tumor cells diffuse VEGF in an attempt to induce angiogenesis (Figure 1). As VEGF travels through the system, it is spread from its current location within its immediate Moore neighborhood. The amount of VEGF at the location (*currentVEGF*) is initially 1 for the hypoxic cell's (x,y,z), with 90% diffusing to neighbors. The amount diffused to an individual neighbor is therefore $0.9 * currentVEGF / (8 * numDimensions + numDimensions - 1)$, and is added to any VEGF already at that location. The diffusion continues from all locations with VEGF greater than the minimum of 0.0001, with $0.9 * currentVEGF$ diffusing among the neighbors. VEGF only disappears from the system when the amount at a particular grid point is below the minimum. Once the chemical reaches a vessel it will induce the creation of a sprout if there is not already one growing from that vessel within $30\mu m$.

Each sprout can grow by five endothelial cells every time step, and we assume that endothelial cells are the size of tumor cells. Sprouts grow by biased random movement based on the gradient of VEGF within the system (Figure 3). They are also limited in that they can only grow in locations where other cells are not already present, and they are not allowed to form loops with the same sprout.

A sprout is not viable and thus does not provide nutrients to surrounding cells until it forms a loop with another sprout or vessel. Once the sprout becomes viable, it will provide nutrients to nearby cells but not to the same extent that a vessel could provide. Instead, the amount of oxygen diffused in total by a sprout (ρ_s) is relative to its length

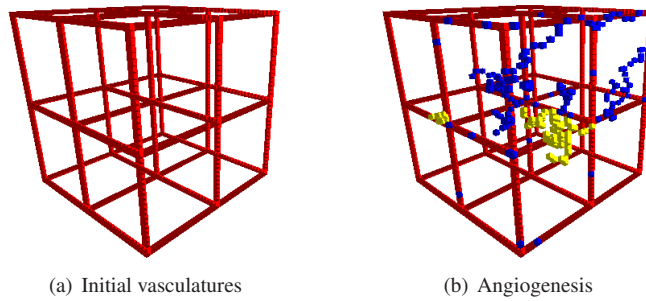


Fig. 3. Modeled vasculatures. (a) The initial vessels capable of providing oxygen to the simulated tissue. (b) Vessel growth due to tumor diffusion of VEGF; yellow are viable vessels that have formed a loop and thus diffuse oxygen, whereas blue are non-viable endothelial cells.



Fig. 4. General growth pattern of modeled cancer cells. Tumor exhibit spheroid growth patterns as well as the expected branching processes. Normal cells and vasculatures are not shown, although they are influencing the tumor’s growth.

(*l*) as seen in Equation 2. This limited nutrient, however, will allow the tumor to grow further, and create more sprouts as it grows as well. The diffusion of this nutrient occurs via an algorithm similar to Algorithm 1, except that the diffusion radius is limited to half of a normal vessel’s diffusion radius.

$$\rho_s = \sum_i^{\text{diffusionRadiusMax/numDimensions}} (\alpha * i) * l/\alpha + 5 \tag{2}$$

4. Results

In all instances the model is simulated on a size 40x40x40 grid. Compartments have height, width, and depth of 20. Normal cells have the following parameters: proliferation rates in one of three ranges (0.05 – 0.15, 0.03 – 0.09, or 0.015 – 0.045), and apoptosis rates within 0.0024 – 0.0048. Cancer cells have the following related parameters: proliferate rates are limited to the range of 0.3 – 0.9, and apoptosis rates are limited to 0.0001 – 0.0002. These values are chosen to represent breast cancer [25]. Angiogenesis follows the above algorithms when enabled in the simulation.

The model is first analyzed in terms of cellular growth and properties in a system lacking angiogenesis. In all of the parameter cases we first see the expected quick growth of a self-sustaining cellular environment. Once a tumor cell is introduced into the environment, the tumors then proliferate at an unchecked rate until they reach the maximum number that can be sustained. The tumor growth pattern is in the expected spheroid growth pattern although we do not explicitly model this behavior [9, 26], including expected branching (Figure 4). Normal cells mostly die due to their lack of nutrients and inability to proliferate when surrounded by tumor cells. An example of this growth pattern can be seen in Figure 5(a).

As expected, cancer cells are able to grow much larger with angiogenesis, which results in normal cells essentially being removed from the system (Figure 5(b)). Angiogenesis enables tumor cells to increase the nutrient supply around the tumor cell cluster, thus increasing their possible size.

We next compare the model to a previously published angiogenesis model by running the simulation with only tumor cells, as our comparison model does not contain normal cells [15]. As with the other model, we start with a single tumor cell, which eventually grows into a tumor that can no longer be sustained by the vasculature. We

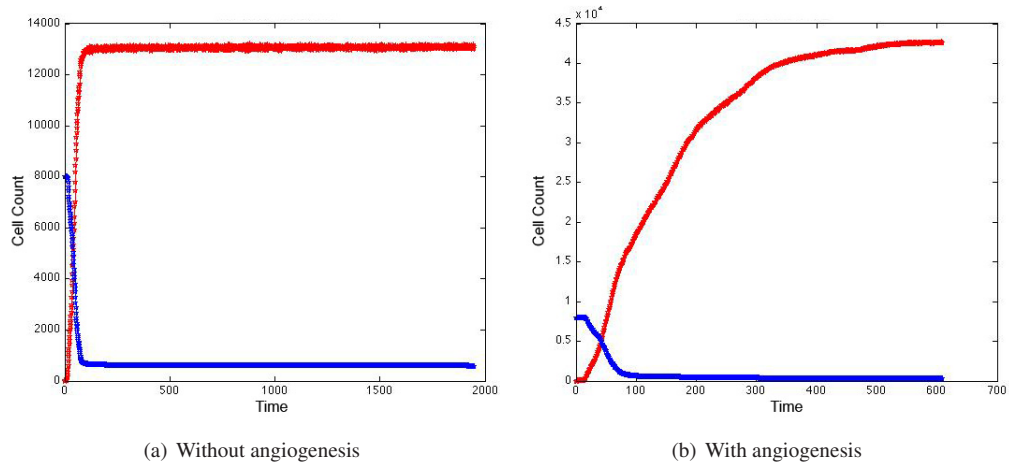


Fig. 5. Change over time in number of cancer (red) and healthy tissue (blue) cells. Note the different axes. (a) When angiogenesis is not activated, cancer cells grow quickly, but are unable to grow large enough to crowd out healthy cells. (b) When angiogenesis is activated, the cancer cells are able to grow much larger and take nutrients and space away from healthy cells such that they basically disappear.

examine the rates of tumor cells, hypoxic cells, and neovascular cells in this model (Figure 6) over time. The rates of tumor growth with and without angiogenesis relate as we would expect, with tumor growth increasing much faster with angiogenesis, reaching 35000 cells in 400 days instead of 15000 cells without angiogenesis (Figure 6(a)). Additionally, the tumor grows in a spheroid pattern with small branchings, which is also expected of tumor development.

After approximately 100 days the number of hypoxic cells begins to increase (Figure 6(b)). Once the vasculature can't sustain tumor growth, hypoxic cells diffuse VEGF and angiogenesis begins. Notice that the increased tumor growth rate corresponds to the increase in neovascular and hypoxic cells. We see an increase in hypoxic cells in both cases, as cells will lack nutrients whether or not the tumor cells can encourage angiogenesis. In the case of no angiogenesis ability, although the number of hypoxic cells increases the overall growth of tumor cells is delayed as the cluster can only proliferate in areas where nutrient is still available. Eventually we start to see a more exponential growth in the case of angiogenesis, showing that the tumor is able to grow but still cannot support all cells.

These results are as we expect to see, and are very similar to the results from [15]. However, the most noticeable differences between our results are the amount of time to see these patterns, as well as the number of tumor cells simulated. These differences may be an artifact from our inclusion of normal tissue cells, showing that to truly model cancer growth we need to include these cells in our simulations.

5. Discussion

We present a new three-dimensional multiscale agent-based model for cancer growth. This model is an improvement over previous models as it explicitly models normal tissue cells in addition to cancer cells. The functioning of cells is probabilistic, with probabilities drawn from the literature and experts in the field. Additionally, the definition of the functioning of a cancer cell is based on the hallmarks of cancer [5]. We also directly model nutrient (oxygen) diffusion from vasculatures, and cancer angiogenesis through the diffusion of VEGF that initiates sprouts from blood vessels. Our methods are novel in comparison to previous angiogenesis models. We are able to abstract the flow of oxygen without losing the details of nutrient availability, VEGF diffusion, or its resulting stimulation of new capillary growth.

Our tumor cells grow in the spheroid shape that is generally expected in cancer growth, whether or not angiogenesis is activated. With angiogenesis tumors are able to grow significantly bigger than without angiogenesis. Our model shows a similar rate of growth of both cells and vasculatures as in the first five phases modeled in [15], despite our discretization of the angiogenesis process. However, our timeline is elongated in comparison. This

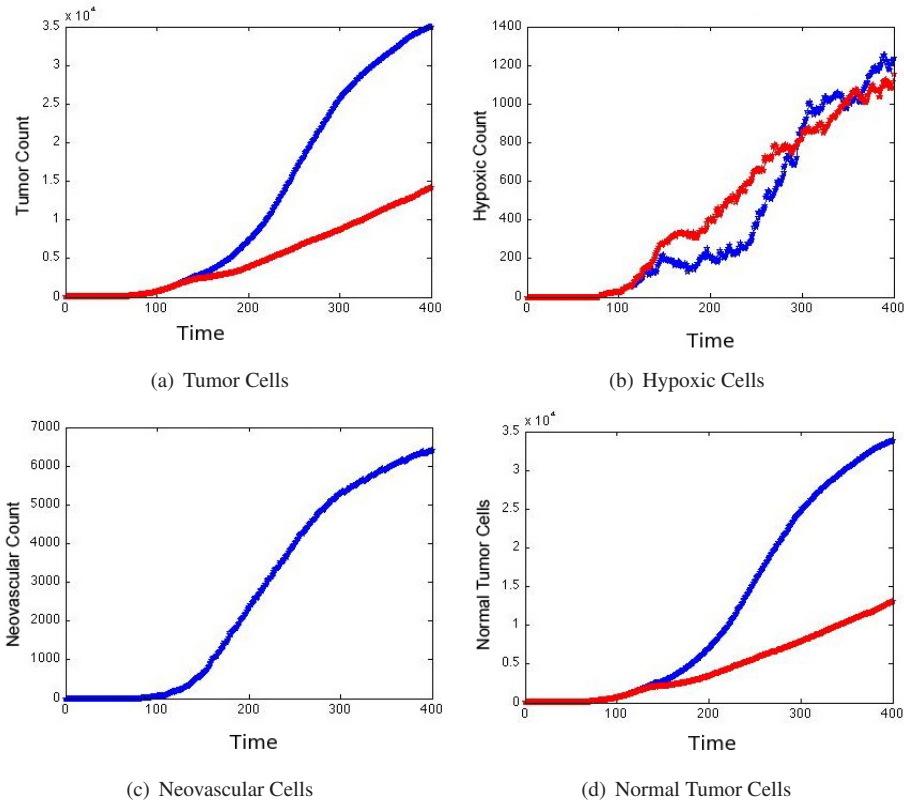


Fig. 6. Change over time of cell counts with (blue) and without (red) angiogenesis: (a) Number of tumor cells, (b) Number of hypoxic (low nutrient) cells, (c) Number of neovascular (new vessel) cells, and (d) Number of non-hypoxic tumor cells. More tumor cells are able to grow with angiogenesis, and eventually there is also more rapid creation of hypoxic cells with angiogenesis. These results resemble the first five phases in [15].

difference may be due to our larger system scale, or may indicate that different parameters may be necessary to the angiogenesis model to change the growth speed.

Our model represents a new variation on multiscale angiogenesis models. As our new discretization and abstraction of the angiogenesis process gives similar results to previous models, we propose that this model and its modeling approach be considered in future tumor growth model development. Being able to discretize nutrient flow and capillary growth will decrease simulation time without sacrificing accuracy. More efficient modeling will allow the study of more complex and larger tumors, in addition to the including the surrounding tissue cells that are currently ignored by most models.

Acknowledgements

The authors would like to thank Joe Jerry, Nava Sieglemann-Danieli, and John Nambu for their guidance on various biological aspects of this work, as well as the conference reviewers for their feedback. The first author would also like to thank Yariv Levy for his feedback.

References

- [1] K. M. Yamada, E. Cukierman, Modeling tissue morphogenesis and cancer in 3d, Cell 130.
- [2] O. Wolkenhauer, C. Auffray, S. Baltrusch, N. Blthgen, H. Byrne, M. Cascante, A. Ciliberto, T. Dale, D. Drasdo, D. Fell, J. E. Ferrell, D. Gallahan, R. Gatenby, U. Gnther, B. D. Harms, H. Herzel, C. Junghanss, M. Kunz, I. van Leeuwen, P. Lenormand, F. Levi, M. Linnebacher, J. Lowengrub, P. K. Maini, A. Malik, K. Rateitschak, O. Sansom, R. Schfer, K. Schrrle, C. Sers, S. Schnell, D. Shibata,

- J. Tyson, J. Vera, M. White, B. Zhivotovsky, R. Jaster, Systems biologists seek fuller integration of systems biology approaches in new cancer research programs, *Cancer Research* 70 (1) (2010) 12–13. doi:10.1158/0008-5472.CAN-09-2676.
- [3] H. Kitano, Systems biology: A brief overview, *Science* 295 (5560) (2002) 1662–1664. arXiv:<http://www.sciencemag.org/content/295/5560/1662.full.pdf>, doi:10.1126/science.1069492. URL <http://www.sciencemag.org/content/295/5560/1662.abstract>
- [4] I. Zechmeister, B. Freiesleben de Blasio, G. Garnett, Hpv-vaccination for the prevention of cervical cancer in austria: a model based long-term prognosis of cancer epidemiology, *Journal of Public Health* 18 (2010) 3–13.
- [5] D. Hanahan, R. A. Weinberg, The hallmarks of cancer, *Cell* 100 (2000) 57–70.
- [6] J. Plotkin, M. A. Nowak, Different effects of apoptosis and dna repair on tumorigenesis, *Journal of Theoretical Biology* 214 (2002) 453–467. doi:10.1006/jtbi.2001.2471.
- [7] T. Lindahl, R. D. Wood, Quality control by dna repair, *Science* 286 (3).
- [8] R. Abbott, *Cancersim: A computer-based simulation of hanahan and weinberg's hallmarks of cancer*, Master's thesis, University of New Mexico (2002).
- [9] L. Zhang, C. Athale, T. S. Deisboeck, Development of a three-dimensional multiscale agent-based tumor model: Simulating gene-protein interaction profiles, cell phenotypes and multicellular patterns in brain cancer, *Journal of Theoretical Biology*.
- [10] S. R. McDougall, A. R. A. Anderson, M. A. J. Chaplain, Mathematical modelling of dynamic adaptive tumour-induced angiogenesis: Clinical implications and therapeutic targeting strategies, *Journal of Theoretical Biology* 241 (3) (2006) 564–589. doi:10.1016/j.jtbi.2005.12.022. URL <http://www.sciencedirect.com/science/article/B6WMD-4J91NR8-1/2/8644ffbaab6cd3ca5e099b22576b975>
- [11] M. A. J. Chaplain, Mathematical modelling of angiogenesis, *Journal of Neuro-Oncology* 50 (2000) 37–51, 10.1023/A:1006446020377. URL <http://dx.doi.org/10.1023/A:1006446020377>
- [12] M. R. Owen, T. Alarcon, P. K. Maini, H. M. Byrne, Angiogenesis and vascular remodelling in normal and cancerous tissues, *Journal of Mathematical Biology* 58 (4-5) (2009) 689–721.
- [13] E. B. Shim, Y.-G. Kwon, H. J. Ko, Computational analysis of tumor angiogenesis patterns using a two-dimensional model, *Yonsei Medical Journal* 46 (2) (2005) 275–283.
- [14] A. L. Bauer, T. L. Jackson, Y. Jiang, A cell-based model exhibiting branching and anastomosis during tumor-induced angiogenesis, *Biophysical Journal* 92 (9) (2007) 3105–3121. doi:10.1529/biophysj.106.101501. URL <http://www.sciencedirect.com/science/article/B94RW-4TR4KB1-P/2/47e6d417197d70233ff79f9bd473089d>
- [15] A. Shirinifard, J. S. Gens, Zaitlen, 3d multi-cell simulation of tumor growth and angiogenesis, *PLoS ONE* 4 (10) (2009) e7190. doi:10.1371/journal.pone.0007190.
- [16] M. Markus, D. Böhm, M. Schmick, Simulation of vessel morphogenesis using cellular automata, *Mathematical Biosciences* 156 (1-2) (1999) 191–206. doi:10.1016/S0025-5564(98)10066-4. URL <http://www.sciencedirect.com/science/article/B6VHX-3W374Y2-9/2/d03620d18d402fe799635911fa3dab5c>
- [17] P. Topa, Dynamically reorganising vascular networks modelled using cellular automata approach, in: *Proceedings of the 8th international conference on Cellular Automata for Research and Industry, ACRI '08*, Springer-Verlag, Berlin, Heidelberg, 2008, pp. 494–499. doi:10.1007/978-3-540-79992-4_64.
- [18] S. M. Peirce, E. J. Van Gieson, T. C. Skalak, Multicellular simulation predicts microvascular patterning and in silico tissue assembly, *The FASEB Journal* 18 (6) (2004) 731–733. doi:10.1096/fj.03-0933fje.
- [19] D. Dréau, D. Stanimirov, T. Carmichael, M. Hadzikadic, An agent-based model of solid tumor progression, in: *Proceedings of the 1st International Conference on Bioinformatics and Computational Biology, BICoB '09*, Springer-Verlag, Berlin, Heidelberg, 2009, pp. 187–198.
- [20] M. M. Olsen, N. Siegelmann-Danieli, H. T. Siegelmann, Robust artificial life via artificial programmed death, *Artificial Intelligence* 172 (2008) 884–898.
- [21] R. C. Allsopp, H. Vaziri, C. Patterson, S. Goldstein, E. V. Younglai, A. B. Futcher, C. W. Greider, C. B. Harley, Telomere length predicts replicative capacity of human fibroblasts, *Proceedings of the National Academy of Sciences of the United States of America* 89 (21) (1992) 10114–10118.
- [22] H. D. Ryoo, T. Gorenc, H. Steller, Apoptotic cells can induce compensatory cell proliferation through the jnk and the wingless signaling pathways, *Developmental Cell* 7 (4) (2004) 491 – 501. doi:10.1016/j.devcel.2004.08.019. URL <http://www.sciencedirect.com/science/article/B6WW3-4DHN7DC-8/2/cef72f5e91f6552d24d5637062093238>
- [23] N. Barkai, B.-Z. Shilo, Variability and robustness in biomolecular systems, *Molecular Cell* 28 (5) (2007) 755–760. doi:10.1016/j.molcel.2007.11.013. URL <http://www.sciencedirect.com/science/article/B6WSR-4RBM5GD-9/2/95f047d342ea349536c09caf92ebd481>
- [24] A. R. Anderson, A. M. Weaver, P. T. Cummings, V. Quaranta, Tumor morphology and phenotypic evolution driven by selective pressure from the microenvironment, *Cell* 127 (5) (2006) 905 – 915. doi:10.1016/j.cell.2006.09.042. URL <http://www.sciencedirect.com/science/article/B6WSN-4MG0YV3-C/2/a27cc76f4b8a02d9087f0607cc2c525f>
- [25] M. M. Olsen, N. Siegelmann-Danieli, H. T. Siegelmann, Dynamic computational model suggests that cellular citizenship is fundamental for selective tumor apoptosis, *PLoS One* 5 (5).
- [26] G. Pettet, C. Please, M. Tindall, D. McElwain, The migration of cells in multicell tumor spheroids, *Bulletin of Math Bio* 63 (2001) 231–257.